Journal of Hazardous Materials 160 (2008) 78–82

Contents lists available at ScienceDirect

Journal of Hazardous Materials

journal homepage: www.elsevier.com/locate/jhazmat

Preparation, characterization and photocatalytic activity of manganese doped TiO_2 immobilized on silica gel

Yuehua Xu*, Bo Lei, Laiqiu Guo, Wuyi Zhou, Youqin Liu

College of Science, South China Agricultural University, Guangzhou 510642, China

ARTICLE INFO

Article history:
Received 18 June 2007
Received in revised form 23 February 2008
Accepted 25 February 2008
Available online 4 March 2008

Keywords:
TiO_2
Silica gel
Doping Mn
Photocatalytic
Methyl orange

ABSTRACT

A series of Mn-TiO_2/SiO_2 (silica gel loaded with manganese doped TiO_2) photocatalysts have been prepared by sol–gel method, and characterized by X-ray diffraction (XRD), scanning electron microscopy (SEM), and X-ray photoelectron spectroscopy (XPS). Photocatalytic activities were enhanced in photocatalytic degradation of methyl orange over Mn-TiO_2/SiO_2. XPS analysis shows that a Ti—O—Si or Ti—O—Mn bond is formed on the surface of photocatalyst. Mn is doped as a mixture of Mn^{2+} and Mn^{3+} on the surface of 1.0 mol% Mn-TiO_2/SiO_2. Mn^{3+} appears to trap electrons and prohibit the electron–hole recombination. The electrons trapped in Mn^{3+} site are subsequently transferred to the adsorbed O_2. As a result, the combination of the electron–hole pair was reduced.

1. Introduction

Photocatalysis is a promising technique for the photocatalytic oxidation of organic pollutants in water. However, practical applications of TiO_2 powder are limited because of problems of separation of fine TiO_2 particles from the treated liquid [1–2]. Many techniques [3–7] were proposed for the immobilization of TiO_2 on solid supports to eliminate the problem of separation of fine TiO_2 particles used after the treatment process and the recycling of the photocatalyst. However, a decrease in efficiency of photocatalytic reactions has been usually observed after immobilization. SiO_2 material has been widely used as supports for TiO_2 [8–10], and many researchers have investigated TiO_2/SiO_2 materials as supports for different metal catalysts with different methods [11], such as wet impregnation technique [12], the atomic layer deposition method [13], etc. However, these metal-TiO_2/SiO_2 were not used as photocatalysts. Moreover, doping transition metal ions have been extensively studied, and it has been shown that the photocatalytic activity of TiO_2 was high after doping manganese ions [14–16]. For the reasons given above a series of Mn-TiO_2/SiO_2 were prepared by sol–gel method, and characterized with XRD, SEM, and XPS. The photocatalytic activity of Mn-TiO_2/SiO_2 for the degradation of a model compound methyl orange, which has been widely investigated by many researchers in the field of photocatalysis, is presented in this paper. Our main concern is to gain higher efficient photocatalysts, which are convenient for recycling, and the description of the chemical and physical properties that could help with a deeper understanding of the photocatalytic mechanism.

2. Experimental

2.1. Preparation of photocatalyst

Series of Mn-TiO_2/SiO_2 with Mn-doped content in the range of 0.1–5.0 mol% were prepared by sol–gel method (as shown in Fig. 1). The preparation was carried out as follows: 30 mL pure alcohol and 2.25 g diethanolamine were added to 7.50 g $Ti(O\text{-}Bu)_4$, and then a required amount of manganese sulfate aqueous solution was added dropwise under stirring for 30 min. After that 0.25 g polyethylene glycol was dissolved into the above sol under continuous stirring for 30 min to obtain reddish sol, and the molar ratio of $Ti(O\text{-}Bu)_4$:EtOH:DEA:PEG4000 is 1:23.32:0.97:0.0028.

The size of commercial SiO_2 (silica gel) is in the range of 75–150 μm. SiO_2 was dipped into the above reddish sol and stirred for 2 h. After vacuum filtration, samples were transferred to an oven and baked at 70 °C. Mn-TiO_2/SiO_2 with Mn-doped sol–gel coating was prepared. The above process was repeated one more time, and Mn-doped TiO_2 sol–gel layer was twice loaded on Mn-TiO_2/SiO_2. The above samples were calcined in air at 600 °C for 2 h, and Mn-TiO_2/SiO_2 with two Mn-TiO_2 coatings was obtained. For comparison, if no manganese sulfate was added, TiO_2/SiO_2 was obtained. In the text all the photocatalysts were labeled as TS (TiO_2/SiO_2), MTS (Mn-TiO_2/SiO_2), and 1.0% MTS (1.0%

* Corresponding author. Tel.: +86 20 85281989; fax: +86 20 85281989.
E-mail address: xuyuehua@scau.edu.cn (Y. Xu).

0304-3894/$ – see front matter © 2008 Elsevier B.V. All rights reserved.
doi:10.1016/j.jhazmat.2008.02.086

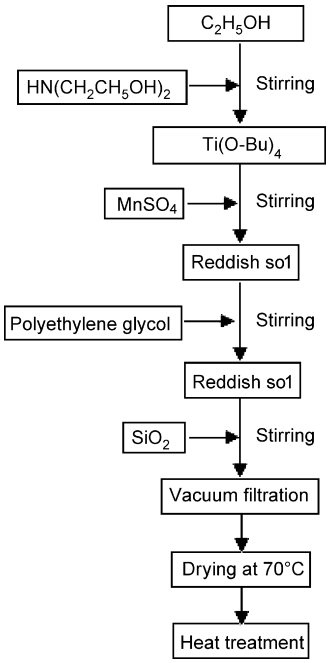

Fig. 1. Preparation flowchart of MTS.

Mn-TiO_2/SiO_2), for the sake of convenience in discussing the results. TiO_2 content in TiO_2/SiO_2 with two coatings is about 5.0 mol%.

2.2. Characterization

The X-ray diffraction (XRD) patterns were obtained at room temperature with a D/Max × IIIA diffractometer (λ = 0.15406 nm). The X-ray photoelectron spectroscopy (XPS) spectra were analyzed by a VG ESCALAB MK II with a pass energy of 20 eV, and the excitation of the spectra was performed using monochromatized Mg Kα radiation. The binding energy (BE) scale was referenced to the energy of the C 1s peak of adventitious carbon, E_B = 284.8 eV. Morphology was observed by scanning electron microscopy (SEM) using a SEMS, Model FEI-XL30, Philips, Holland.

2.3. Photocatalytic activity

Aqueous slurries were prepared by adding 0.40 g photocatalyst to 350 mL methyl orange aqueous solution at 15 mg L^{-1}. Irradiations were performed with a 250 W high-pressure mercury lamp. A schematic diagram of the used reactor is shown in Fig. 2. The aqueous slurries were stirred and bubbled with oxygen for 30 min prior

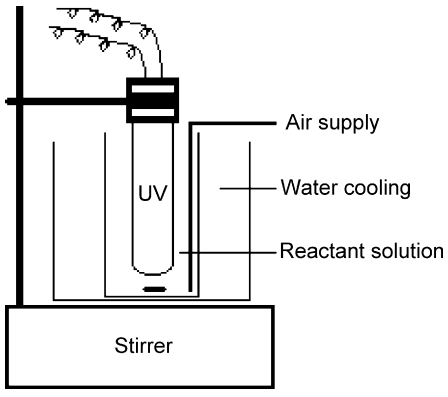

Fig. 2. Schematic diagram of the used reactor.

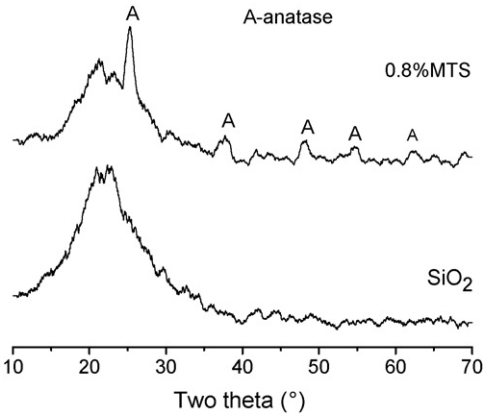

Fig. 3. XRD spectra of SiO_2 and 0.8% MTS.

to the irradiation. At 5 min intervals, the suspension was extracted and centrifuged to separate the photocatalyst particles. The filtrates were analyzed with a spectrophotometer by measuring their absorbance at 490 nm.

3. Results and discussion

3.1. XRD analysis

X-ray diffraction patterns of SiO_2 and 0.8% MTS are shown in Fig. 3. The X-ray diffraction peak at 25.3° corresponds to the characteristic peak of crystal plane (1 0 1) of anatase, and the peak at 27.6° corresponds to the characteristic peak of crystal plane (1 1 0) of rutile. The XRD pattern of 0.8% MTS shows anatase peaks (2θ = 25.28°, 37.74°, 48.34°, 54.58°), so anatase is the main phase present for TiO_2. The XRD pattern of 0.8% MTS indicates that no characteristic peaks of manganese species are found because of a low manganese content.

3.2. SEM analysis

Fig. 4 presents SEM photographs of support and photocatalysts. Fig. 4a shows that the surface of commercial SiO_2 was slick. Fig. 4b and c show SEM photographs of TS and MTS, respectively, and they are similar. A layer of TiO_2 or Mn-TiO_2 was obvious on the surface of SiO_2.

3.3. XPS analysis

Fig. 5 shows XPS survey spectra of TS and 1.0% MTS photocatalyst, respectively. It can be seen clearly that there are Ti, O, C and Si peaks on the TS and 1.0% MTS surface. Moreover, there is Mn peak on surface of 1.0% MTS. The photoelectron peak for C 1s is probably attributed to the contamination caused by specimen handing or pumping oil from the XPS instrument itself. Because another weak C 1s peak at 288.6 eV, which is due to the existence of residual carbon from precursor solution [17–18], was not detected in XPS survey spectra for the surface of TS and 1.0% MTS.

The representative XPS bands of O 1s and Mn 2p are shown in Figs. 6–8, respectively, and the corresponding binding energies and the full width at half maximum (FWHM) values are summarized in Table 1.

XPS spectra (not shown here) of Ti 2p show a narrow and symmetrical Ti 2p peak, the binding energy of Ti $2p_{3/2}$ for TS and 1.0% MTS is 459.66 eV and 458.85 eV, respectively. This result indicates that Ti mainly exists as the chemical state of Ti^{4+} on the surface of TS and 1.0% MTS photocatalyst. The binding energy of the Ti $2p_{3/2}$ band in the case of TS and 1.0% MTS samples is higher than that of the pure

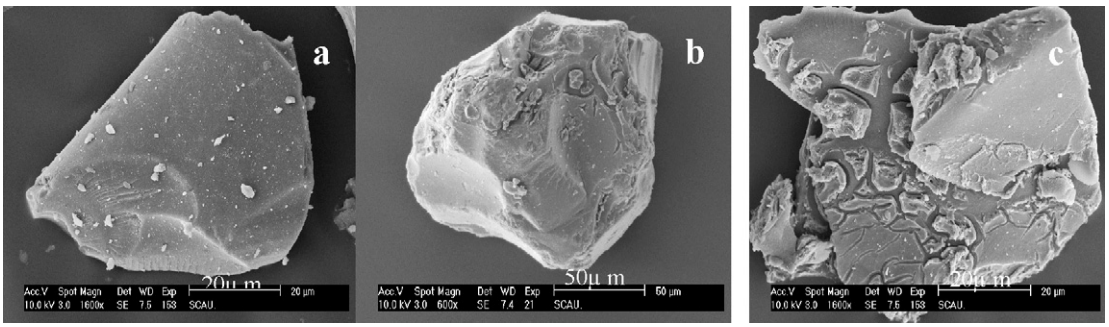

Fig. 4. SEM photographs of support and photocatalysts: (a) SiO_2, (b) TS, and (c) 0.5% MTS.

Table 1
XPS fitting data for TS and 1.0% MTS.

Photocatalyst	Ti ($2p_{3/2}$)	Mn ($2p_{3/2}$)	Si (2p)	O 1s (SiO_2)	O 1s (OH)	O 1s (Ti—O or Mn—O)
TS						
BE (eV)	459.65		103.83	533.40	531.62	530.31
FWHM	1.86		3.03	2.17	2.32	3.00
At. (%)	5.27		16.71	47.83	18.54	11.64
1.0% MTS						
BE (eV)	458.85	641.45	103.78	533.33	531.63	529.83
FWHM	1.88	0.62	3.11	2.26	2.38	2.05
At. (%)	5.25	0.68	15.09	46.66	19.62	12.69

FWHM: full width at a half of the maximum height of peaks. BE: binding energy.

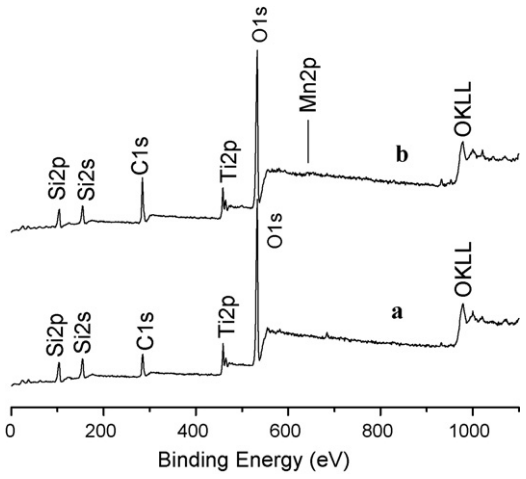

Fig. 5. XPS survey spectra for the surface of (a) TS and (b) 1.0% MTS.

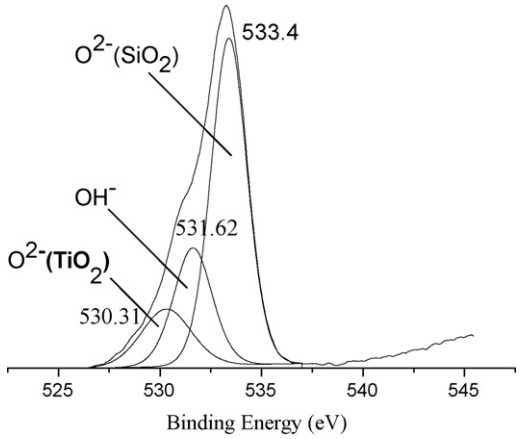

Fig. 6. O 1s curves fitted of TS.

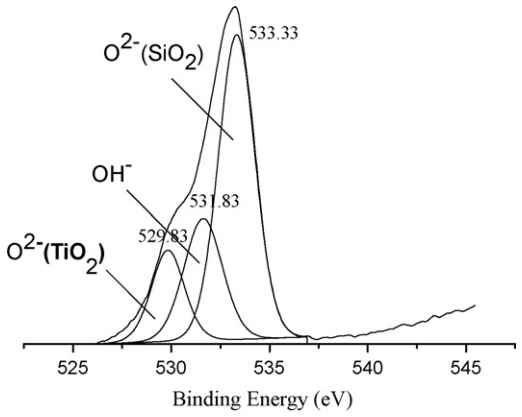

Fig. 7. O 1s curves fitted of 1.0% MTS.

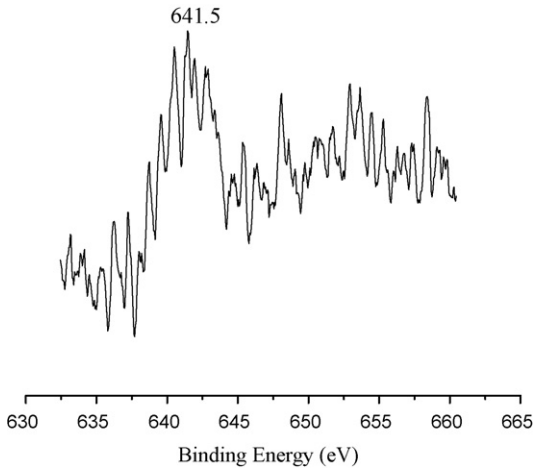

Fig. 8. XPS spectrum of Mn 2p for 1.0% MTS.

TiO_2 (458.0–458.5 eV) [12,19–21]. In general, the core-level shifts are assigned to changes in the electronegativities (Pauling term), in the ionicities (Madelung term) and on the final states (relaxation term) in the environment of the photoionized atom [12]. The Ti is less electronegative than Si (Pauling values Ti: 1.5, Si: 1.8), which reflects more ionic character for TiO_2. Garbassi and Balducci [8] and Keränen et al [13] reported that the binding energy of 459.5 eV is connected with the location of Ti atoms on tetrahedral sites, while the energy of about 458.5 eV indicates the presence of octahedrally coordinated titanium in the sample. These results indicate a change in coordination from octahedral to tetrahedral, so the shift towards higher side could be attributed to the change in the coordination number of titanium by the formation of a Ti—O—Si or Ti—O—Mn bond. The binding energy (BE) of the Si 2p peaks is at 103.83 eV for TS and 103.78 eV for 1.0% MTS, these agree well with the values reported in the literatures [8,12–13].

The O 1s patterns of XPS of TS and 1.0% MTS are shown in Fig. 6 and Fig. 7, respectively. It can be seen that both O 1s XPS spectra exhibit single-lobed peaks, and the peaks are asymmetric (the left sides are wider than the right), indicating that the different oxygen contributions exist on the photocatalyst surface. The O 1s peaks could be fitted into three peaks, and the main contributions are attributed to Si—O in SiO_2. The other two kinds of oxygen contributions are Ti—O in photocatalysts and the hydroxyl groups, respectively [17,22–23]. Consequently there are three oxygen contributions existing on the photocatalyst surface, including Si—O in SiO_2, Ti—O in TiO_2, and the hydroxyl groups. As shown in Table 1, the Ti content of TS is almost same as that of 1.0% MTS. However, for TS the percentage of the hydroxyl group and lattice oxygen is smaller than 1.0% MTS. The Ti is less electronegative than Si (Pauling values Ti: 1.5, Si: 1.8), which reflects more ionic character for TiO_2. This means that the Lewis acidity could be predicted when a Ti cation is incorporated in to a more covalent SiO_2 matrix at the site of the substituted ion [12]. The increase of Lewis acidity would form more hydroxyl groups on the surface of photocatalyst [24]. The formation of hydroxyl groups serving as hole trapped sites inhibit the recombination of negative electrons with positive holes, and form hydroxyl radical:

$$OH^{\bullet -} + h^+ \rightarrow OH \quad (1)$$

Therefore, the formation of hydroxyl radicals is from the reaction between hydroxide ion trapped on the surface and the positive hole.

Mn 2p spectrum for 1.0% MTS is presented in Fig. 8. The binding-energy value of the Mn $2p_{3/2}$ peak is 641.5 eV. According to the literatures [25–26], this value indicates that Mn is present as a mixture of Mn^{2+} and Mn^{3+} on the surface of 1.0% MTS.

3.4. Photocatalytic results

Fig. 9 shows the photocatalytic activity for methyl orange photocatalytic degradation over TS and MTS. Although methyl orange can be degraded under UV light, it has been widely investigated as a model compound by many researchers in the field of photocatalysis. Compared to UV light alone, methyl orange degraded slowly when SiO_2 existed in reactant solution under UV light. This may be explained by the fact that the UV light is probably screened by SiO_2 particles, which is an insulator, in the solution. It is shown that the photocatalytic activity of TS enhanced after manganese doping. The photocatalytic activity of MTS increases with Mn content and then diminishes when the Mn-doped content is up to 0.5%. When Mn-doped content reaches 0.8%, the photocatalytic reactivity is similar to that of TS. Compared to TS, the high photocatalytic activity of MTS would be due to the variable valence of manganese [15]. Because Mn^{2+} and Mn^{3+} coexist on the surface of 1.0% MTS photocatalyst, metal ions are the acceptors of electrons, and Mn^{3+} can trap electrons in TiO_2 conduction band. So Mn^{3+} should trap electrons and prohibit electron–hole recombination. That is, the lower the recombination efficiency of the electron–holes is, the higher the quantum efficiency of the photons will be [16]. Moreover, the electrons trapped in Mn^{3+} site are subsequently transferred to the adsorbed O_2, and decrease the recombination rate of the electron–hole pair. During the transfer processes of trapped electrons to O_2 adsorbed on the reaction interface, a sequence of reactions can be expressed by the following set of equations, because Mn^{2+} and Mn^{3+} coexist in 1.0% MTS:

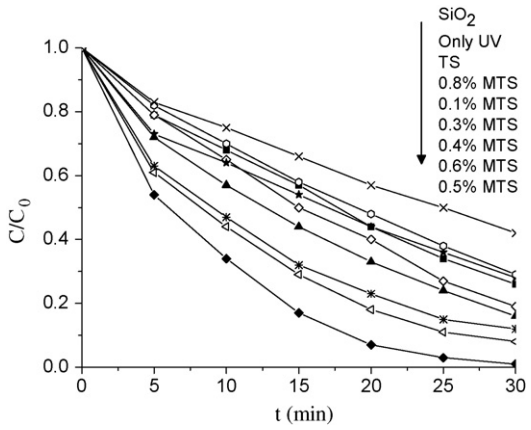

Fig. 9. Comparison of the photocatalytic activity.

$$Mn^{3+} + e_{cb}{}^- \rightarrow Mn^{2+} \quad (2)$$

$$Mn^{2+} + O_{ads} \rightarrow Mn^{3+} + O_{ads}{}^- \quad (3)$$

Only electron trapped on photocatalyst surface is transferred to O_2 adsorbed on the reaction interface, electrons can be separated from holes. Otherwise, they can still recombine with holes. The process of electrons trapped and the transfer of trapped electrons to O_2 adsorbed on the reaction interface inhibits electron–hole recombination. Moreover, hydroxyl groups trap holes, generating highly reactive hydroxyl radicals. So the photogenerated electron and hole are effectively separated. However, it becomes the recombination center of electron–hole pair, when manganese doped content increases further. It is thought generally that the thickness of the space charge layer (W) decreases with an increase in dopant content. When the value of W approximates that of the penetration depth of the light into the solid, all the photons absorbed generate electron–hole pairs that are efficiently separated [19]. Consequently, it is understandable that an optimal Mn-doped content exists.

4. Conclusion

MTS shows anatase peaks. A Ti—O—Si or Ti—O—Mn bond is formed on the surface of photocatalysts and for TS the percentage of the hydroxyl group and lattice oxygen is smaller than 1.0% MTS. Mn is present as a mixture of Mn^{2+} and Mn^{3+} on the surface of 1.0% MTS, and Mn^{3+} appears to trap electrons and inhibit the electron–hole recombination. The electrons trapped in Mn^{3+} site are subsequently transferred to the surrounding adsorbed O_2, and hence extending the lifetime of the electron–hole pair. In this way, Mn^{3+} of MTS traps photoinduced electrons and surface hydroxyl group traps photoinduced hole, which forms hydroxyl radical.

Acknowledgements

The authors would like to thank Guangdong Science & Technology Development Foundation (2007B030103019) and South China Agricultural University (2006X017) for financial supports to this work.

References

[1] I. Sopyan, M. Watanabe, S. Murasawa, K. Hashimoto, A. Fujishima, An efficient TiO_2 thin-film photocatalyst: photocatalytic properties in gas-phase acetaldehyde degradation, J. Photochem. Photobiol. A: Chem. 98 (1996) 79.
[2] A. Rachel, M. Subrahmanyam, P. Boule, Comparison of photocatalytic efficiencies of TiO_2 in suspended and immobilised form for the photocatalytic degradation of nitrobenzenesulfonic acids, Appl. Catal. B: Environ. 37 (2002) 301.
[3] E. Carpio, P. Zúñiga, S. Ponce, J. Solis, J. Rodriguez, W. Estrada, Photocatalytic degradation of phenol using TiO_2 nanocrystals supported on activated carbon, J. Mol. Catal. A: Chem. 228 (2005) 293.
[4] M. Mohseni, Gas phase trichloroethylene (TCE) photooxidation and byproduct formation: photolysis vs. titania/silica based photocatalysis, Chemosphere 59 (2005) 335.
[5] M.C. Hidalgo, D. Bahnemann, Highly photoactive supported TiO_2 prepared by thermal hydrolysis of $TiOSO_4$: Optimization of the method and comparison with other synthetic routes, Appl. Catal. B: Environ. 61 (2005) 259.
[6] M. Keshmiri, M. Mohseni, T. Troczynski, Development of novel TiO_2 sol–gel-derived composite and its photocatalytic activities for trichloroethylene oxidation, Appl. Catal. B: Environ. 53 (2004) 209.
[7] G. Balasubramanian, D.D. Dionysiou, M.T. Suidan, I. Baudin, J.-M. Laîné, Evaluating the activities of immobilized TiO_2 powder films for the photocatalytic degradation of organic contaminants in water, Appl. Catal. B: Environ. 47 (2004) 73.
[8] F. Garbassi, L. Balducci, Preparation and characterization of spherical TiO_2-SiO_2 particles, Microporous Mesoporous Mater. 47 (2001) 51.
[9] K.Y. Jung, S.B. Park, Enhanced photoactivity of silica-embedded titania particles prepared by sol–gel process for the decomposition of trichloroethylene, Appl. Catal. B: Environ. 25 (2000) 249.
[10] S.-S. Hong, M.S. Lee, S.S. Park, G.-D. Lee, Synthesis of nanosized TiO_2/SiO_2 particles in the microemulsion and their photocatalytic activity on the decomposition of *p*-nitrophenol, Catal. Today 87 (2003) 99.
[11] J.R. Grzechowiak, I. Szyszka, J. Rynkowski, D. Rajski, Preparation, characterisation and activity of nickel supported on silica-titania, Appl. Catal. A 247 (2003) 193.
[12] B.M. Reddy, B. Chowdhury, P.G. Smirniotis, An XPS study of the dispersion of MoO_3 on TiO_2-ZrO_2, TiO_2-SiO_2, TiO_2-Al_2O_3, SiO_2-ZrO_2, and SiO_2-TiO_2-ZrO_2 mixed oxides, Appl., Catal. A 211 (2001) 19.
[13] J. Keränen, C. Guimon, E. Iiskola, A. Auroux, L. Niinistö, Atomic layer deposition and surface characterization of highly dispersed titania/silica-supported vanadia catalysts, Catal. Today 78 (2003) 149.
[14] L.-R. Feng, S.-J. Lu, F.-L. Qiu, Influence of transition elements dopant on the photocatalytic activities of nanometer TiO_2, Acta Chimica. Sin. 60 (2002) 463.
[15] S.-X. Wu, Z. Ma, Y.-N. Qin, X.-Z. Qi, Z.-C. Liang, Photocatalytic redox activity of doped nanocrystalline TiO_2, Acta Physico-Chimica Sinica 20 (2004) 138.
[16] X.-C. Song, Y.-F. Zheng, H.-Y. Yin, G.-S. Cao, Synthesis and characterization of transition element substituted titanate nanotubes, Acta Physico-Chimica Sinica 21 (2005) 1076.
[17] J.C. Yu, J. Yu, J. Zhao, Enhanced photocatalytic activity of mesoporous and ordinary TiO_2 thin films by sulfuric acid treatment, Appl. Catal. B: Environ. 36 (2002) 31.
[18] J.C. Yu, J. Yu, L. Zhang, W. Ho, Enhancing effects of water content and ultrasonic irradiation on the photocatalytic activity of nano-sized TiO_2 powders, J. Photochem. Photobiol. A: Chem. 148 (2002) 263.
[19] Y.H. Xu, H.R. Chen, Z.X. Zeng, B. Lei, Investigation on mechanism of photocatalytic activity enhancement of nanometer cerium-doped titania, Appl. Surf. Sci. 252 (2006) 8565.
[20] J.A. Navío, G. Colón, M. Macías, C. Real, M.I. Litter, Iron-doped titania semiconductor powders prepared by a sol–gel method. Part I: synthesis and characterization, Appl. Catal. A 177 (1999) 111.
[21] C. Beck, T. Mallat, T. Bürgi, A. Baiker, Nature of active sites in sol–gel TiO_2-SiO_2 epoxidation catalysts, J. Catal. 204 (2001) 428.
[22] V.I. Pârvulescu, S. Boghosian, V. Pârvulescu, S.M. Jung, P. Grange, Selective catalytic reduction of NO with NH_3 over mesoporous V_2O_5-TiO_2-SiO_2 catalysts, J. Catal. 217 (2003) 172.
[23] L. Wicikowski, B. Kusz, L. Murawski, K. Szaniawska, B. Susła, AFM and XPS study of nitrided TiO_2 and SiO_2-TiO_2 sol–gel derived films, Vacuum 54 (1999) 221.
[24] N. Economidis, R.F. Coil, P.G. Smirniotis, Catalytic performance of $Al_2O_3/SiO_2/TiO_2$ loaded with V_2O_5 for the selective catalytic reduction of NO_x with ammonia, Catal. Today 40 (1998) 27.
[25] R.J. Iwanowski, M.H. Heinonen, E. Janik, X-ray photoelectron spectra of zinc-blende MnTe, Chem. Phy. Lett. 387 (2004) 110.
[26] Y. Cai, L. Chou, B. Zang, J. Zhao, S. Li, Selective conversion of CH_4 and CO_2 to C_2 hydrocarbons over Mn-CaO catalysts. II. Catalysts characterization and mechanism deduce, J. Mol. Catal. (China) 19 (2005) 327.